A counterintuitive method for slowing down an analyte in a nanopore and its application to polymer sequencing

G. Sampath

Abstract. A major obstacle in nanopore-based polymer sequencing and analysis is the high speed of translocation of an analyte (nucleotide, DNA, amino acid (AA), peptide) through the pore; it currently exceeds available detector bandwidth. Except for one method that uses an enzyme motor to sequence DNA, attempts to resolve the problem satisfactorily have been unsuccessful. Here a counterintuitive method based on *reversing the pore voltage* and/or *increasing the mobility* of some analytes is described. A simplified Fokker-Planck model shows increases in translocation times of 10s of ms for single nucleotides and AAs. More realistic simulations show that a bi-level positive-negative voltage profile can trap an analyte inside the pore for ~1 ms and thereby enable detection of the four nucleotides and 20 proteinogenic AAs with a low bandwidth. While the bi-level voltage profile also reduces the ionic pore current, other methods, such as optical, that do not depend on ionic current blockades to detect an analyte, can take advantage of the slowdown method given here. This is a potentially viable solution to a problem that has prevented nanopore-based polymer sequencing methods from realizing their full potential.

1. Introduction

In recent years nanopores have emerged as an alternative to established and developing methods of polymer sequencing and analysis [1]. Nanopore sequencing is based on translocating a polymer through a nano-sized pore in an electrolytic cell (e-cell) and using the size of the resulting current blockade (or other methods based on optical labeling) to identify successive monomers. Nanopores are on the way to becoming a viable alternative for DNA sequencing [2]; nanopore protein sequencing is yet to show a similar degree of success [3]. Methods reported include theoretical ones [4,5], practical investigations [6-8], and molecular dynamics simulations [9].

The nanopore approach faces three major problems: 1) The polymer translocates through the pore at a higher rate than the detector's bandwidth can handle; 2) It is hard to distinguish among monomers based on just the blockade level, as different monomers are often physically and/or chemically similar; 3) The blockade level must exceed the noise picked up by the detector. An effective solution to the first problem will also reduce high frequency noise, which serves to mitigate the third problem. A range of slowdown methods have been reported [10-16]; a recent review can be found in [17]. Except for the solution in [16], which uses an enzyme motor to sequence DNA, a more general solution to the problem remains elusive. The second problem, namely separation of the 20 AAs in measurement, is addressed later. A fourth, less severe, problem is that of delivering the analyte from the top of the *cis* chamber of the e-cell to the pore entrance. One recent solution to this is based on the use of nanopipettes to deliver single molecules to desired locations [18].

The present work

Here a counterintuitive method for slowing down an analyte in a nanopore is introduced. It is based on reversing the voltage across the pore and increasing the mobility of an analyte if appropriate. This is the opposite of conventional methods that may be aimed at decreasing the voltage and/or decreasing analyte mobility by using a high viscosity solution. A simplified Fokker-Planck model of analyte translocation in the method presented here shows that significant increases in translocation times, up from tens of nanoseconds to tens of milliseconds, for the four nucleotides (dAMP, dTMP, dCMP, dGMP) and the 20 AAs are possible. This conclusion is supported by simulations that are more realistic than the model and are based on a bi-level voltage profile across the nanopore. Potential solutions to the second and fourth problems are discussed toward the end.

2. A Fokker-Planck model of analyte translocation through a nanopore.

Consider an e-cell with *cis* and *trans* chambers filled with an electrolyte (like KCl) and separated by a thin membrane containing a nano-sized pore (Figure 1a, 1c). When a voltage V (*cis* negative to *trans* positive) is applied across the membrane (Figure 1b) the solution is ionized; Cl- ions flow from *cis* to *trans* through the pore, K+ ions from *trans* to *cis*, An analyte molecule introduced into *cis* will flow in a direction based on the electrical charge it carries. Thus the four nucleotides dAMP, dTMP, dCMP, and dGMP that make up DNA carry approximately the same amount of negative charge and go from *cis* to *trans*. The 20 amino acids carry different amounts of charge, equal to $C_{mult}q$, where C_{mult} is a multiplier that varies between 0 and ±2 and depends on the pH level of the solution, and q is the electron charge. The exact value of C_{mult} can be calculated with the Henderson-Hasselbalch (H-H) equation [19]; see Supplement for the details.

The 20 AAs can be divided into six equivalence classes based on their charge multipliers:

$$\mathbf{AA} = \{ \{A,N,Q,G,I,L,M,F,P,S,T,W,V\}, \{R,K\}, \{D,E\}, \{C\}, \{H\}, \{Y\} \} \quad (1)$$

Two AAs are in the same class if their charge multipliers are the same or nearly so. This classification reduces the number of AAs that have to be examined when studying methods to increase their translocation times in a nanopore.

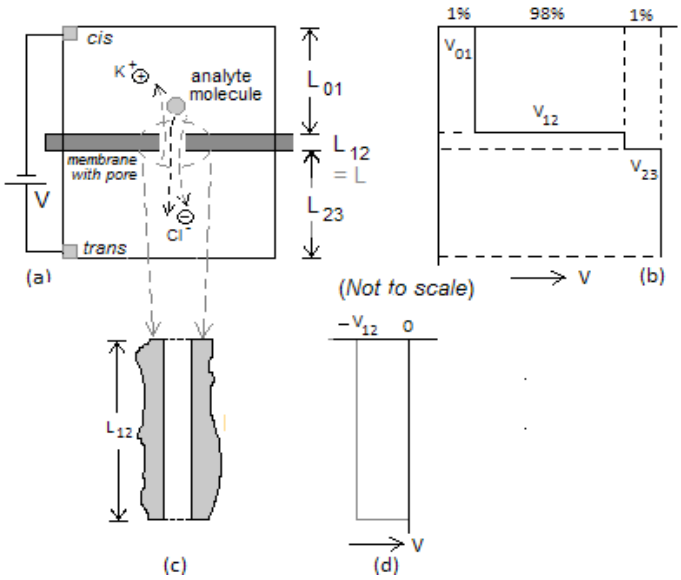

Fig. 1 Schematic of electrolytic cell (e-cell); membrane containing nanopore separates *cis* and *trans* chambers containing salt (KCl) solution. (a) Ionic current flow in e-cell is due to K^+ and Cl^- ions; analyte translocating through pore causes reduction in open pore current; (b) 98% of voltage V applied between *cis* and *trans* drops across pore; (c) Enlarged view of pore of length L_{12}; (d) Negative V across pore in (c)

In the absence of a transmembrane voltage all analytes diffuse through the solution, with the direction of transport determined by boundary conditions. Regardless of the direction of current flow the analyte causes a reduction or blockade in the normal pore current. Here a Fokker-Planck (F-P) equation is used to model analyte motion in the e-cell in Figure 1a and compute the dwell/translocation time of an analyte in/through the pore. Such models have been widely used in the study of DNA and peptide translocation through a nanopore, an example is [20]. The mathematical formulation of the problem is given in the Supplement; only the essential features of the model are presented here.

To start with, a one-dimensional approximation is applied to the nanopore in Figure 1a over the segment $0 \le z \le L_{12}$ over time $t \ge 0$. An analyte is assumed to be a particle that is released at $z = 0$, $t = 0$; reflected at $z = 0$, $t > 0$; and captured at $z = L_{12}$, $t > 0$. The trajectory of the analyte as it passes through the pore is described by the function G(z,t):

$$\partial G/\partial t + vz\, \partial G/\partial z = D\, \partial 2G/\partial z2, \qquad z \in [0, L{=}L_{23}] \tag{2}$$

with the following initial and boundary value conditions:

1) The particle is released at $z = 0$ and time $t = 0$:

$$G(0,t{=}0) = \delta(z) \tag{3}$$

2) The particle is captured at $z = L$:

$$G(L,t) = 0 \tag{4}$$

3) The particle is reflected at $z = 0$:

$$D\, \partial G(z,t)/\partial z\, |_{z=0} = v_z\, G(z,t) \tag{5}$$

Let T be the time of translocation of an analyte through the pore and E(T) its mean. The latter is given by

$$E(T) = (L^2/\mu V_{12})[1 - (1/\alpha)\,(1 - e^{-\alpha})], \qquad \alpha \neq 0 \tag{6a}$$
$$= L^2/2D, \qquad \alpha = 0 \tag{6b}$$
$$\alpha = v_z L/D = \mu V_{12}/D \tag{6c}$$

Equation 6b corresponds to pure diffusion ($\alpha = 0$). In the above, D is the diffusion constant, μ is the analyte mobility, and v_z is the drift velocity through the pore. They are given by

$$D = k_B T_R/6\pi\eta R_{hyd} \qquad \mu = C_{mult} q/6\pi\eta R_{hyd} \qquad v_z = \mu V_{12}/L \tag{7 a,b,c}$$

where k_B = Boltzmann constant (1.3806×10^{-23} J/K), T_R = room temperature (298° K), η = solvent viscosity (0.001 Pa.s for water), R_{hyd} = hydrodynamic radius of the analyte molecule (Å = 10^{-10} m), q = electron charge (-1.619×10^{-19} coulomb), and C_{mult} = charge multiplier for the analyte. C_{mult} is calculated with the H-H equation (see Supplement).

Two cases may be considered.

Case 1: $\alpha >> 0$. In this case $e^{-\alpha} \rightarrow 0$ and Equation 6a reduces to

$$E(T) \rightarrow L^2/\mu V_{12} \qquad (8)$$

One possible way to increase E(T) is to decrease the mobility μ by increasing η (Equation 7b). Practical reductions in μ are typically one to two orders of magnitude [10-13].
Case 2: $\alpha << 0$. With large negative α the exponential term $e^{-\alpha}$ (= $e^{|\alpha|}$) dominates the factor inside the square brackets on the right side of Equation 1a. Then

$$E(T) \approx (L^2/\mu V)\, e^{|\alpha|}/|\alpha| \approx (L^2 D/\mu^2 V^2)\, e^{|\mu V/D|} \qquad (9)$$

Equation 4 shows that with *a linear increase in μ the $e^{|\alpha|}$ term in the numerator increases exponentially, while the denominator increases only as μ^2. Thus reversing V and increasing μ can, in theory, significantly increase the translocation time*.

Table 1 shows translocation times for four nucleotides (dAMP, dTMP,DCMP, and dGMP) for a nanopore of length 10 nm and diameter 3 nm.

Table 1. Translocation times for the four nucleotides in DNA for different pore voltages, positive and negative. Gray level of background of data cells decreases with increasing translocation times.

Trans-membrane voltage	**Translocation time through pore**			
	dAMP	dTMP	dCMP	dGMP
-0.5	42.2 ms	41.3 ms	60.9 ms	42.4 ms
-0.4	1.34 ms	1.32 ms	1.78 ms	1.35 ms
-0.3	48.6 μs	47.7 μs	59.1 μs	49.0 μs
-0.2	2.22 μs	2.18 μs	2.48 μs	2.24 μs
0	27.9 ns	27.5 ns	27.5 ns	28.3 ns
0.2	6.25 ns	6.17 ns	6.05 ns	6.35 ns
0.3	4.37 ns	4.31 ns	4.22 ns	4.44 ns
0.4	3.36 ns	3.31 ns	3.24 ns	3.41 ns
0.5	2.72 ns	2.68 ns	2.63 ns	2.76 ns

Table 2 shows translocation times for five of the 20 AAs for different values of V and pH. The AAs in the first column of Table 3 represent their equivalence class.

Table 2. Translocation times of analytes as a function of solution pH, analyte mobility, and negative pore voltage. Cases in which translocation times are in the millisecond range are shown with gray background.

Analyte	Solution pH	Mobility (m^2/Vs)	V (volt)	Translocation time (ms) through pore	V (volt)	Translocation time (ms) through pore
Alanine	11	3.05×10^{-8}	0.5	1.55×10^{-6}	-0.5	10.2
Arginine	7	-2.36×10^{-8}	0.5	30.00	-0.5	2.01×10^{-6}
Aspartic Acid	7	2.82×10^{-8}	0.5	1.68×10^{-6}	-0.5	26.6
Cysteine	9	2.95×10^{-8}	0.5	1.61×10^{-6}	-0.5	22
Histidine	11	2.32×10^{-8}	0.5	2.04×10^{-6}	-0.5	13.3
Tyrosine	11	4.4×10^{-8}	0.3	1.81×10^{-6}	-0.3	209

3. A bi-level voltage profile to trap an analyte for extended periods of time

The F-P model above considers the pore in isolation and assumes that it is reflective on the inside. The pore, however, is an integral part of an e-cell to which an analyte is added at the top of the *cis* chamber; the latter behaves like a reflective boundary. With V set to the normal polarity (*cis* negative, *trans* positive), a negatively charged analyte diffuses through *cis* to the pore entrance, thereafter it translocates through the pore into *trans*. This latter behavior can be viewed as if the analyte originated from the top of the pore; the translocation time is then given by Equation 8 with $\alpha >> 0$ above (Case 1). This time is the usual low one of the order of a few (10-100) nanoseconds and is normally beyond the capability of the detector.
In what follows, the analyte is assumed to be negatively charged (for example dAMP or glutamic acid). The development can be carried over to positively charged analytes (such as arginine or cysteine) with a systematic change of sign.

Now consider reversing the voltage across the pore. For the F-P model to be applicable, two conditions need to be satisfied:
Condition 1: The analyte must translocate to the entrance of *cis* without being lost to diffusion and enter the pore; and
Condition 2: The pore entrance must behave, at least approximately, like a reflector to an analyte (Equation 4) after the latter enters the pore, and the analyte should not regress into *cis* and diffuse away. This can be written in two parts: a) The analyte must be able to enter the pore before it experiences the decelerating effect of a negative electric field; and b) After entering the negative field the analyte must remain inside the pore for a sufficiently long time to allow its detection; this is contingent on *2a* being satisfied.

For now assume that Condition 1 can be satisfied by using an appropriate method to drive the analyte into the pore; this aspect is discussed later.

Consider what happens when a negative voltage is applied across the full pore. At the *cis*-pore boundary: the analyte experiences a strong negative electric field inside the pore and a much weaker one in *cis*. As a result the analyte will not be able to go too far into the interior of the pore. Condition 2 can be satisfied if a bi-level pore voltage is used with normal polarity over the pore segment [0,aL), $0 \le a < 1$, and the opposite polarity over [0,(1-a)L], with appropriate values of a and V. Such a voltage profile must move the analyte away from the *cis*-pore boundary and far enough into the pore so that the dwell time inside is increased considerably. Figure 2 shows such a profile, which is written as (positive voltage segment, voltage over conducting layer (= 0), negative voltage segment), for example (0.35,0,-0.5). The analyte is only required to be inside the pore for a sufficiently long time, it is not necessary that it fully translocate through the pore into *trans*. In the latter case, following detection the analyte can always be pushed out with an appropriate value of voltage, and the next analyte transferred into *cis*. It is shown below that with a = 0.5 and suitable values of V_{121} and $-V_{122}$ the analyte can be trapped inside the pore for ~1 ms. A detection bandwidth of just a few (1-10) Khz would then be sufficient to detect the trapped analyte.

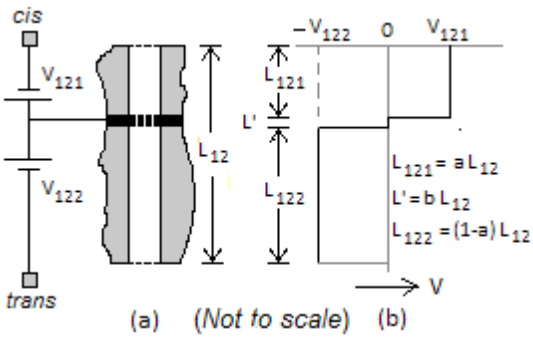

Fig. 2 (a) Two pores in tandem with different voltages across each; (b) Positive voltage V_{121} across pore of length $L_{121} = aL_{12}$, negative voltage V_{122} across pore of length $L_{122} = (1-a)L_{12}$; $0 \le a \le 1$.

A rough estimate of the expected translocation time $E_{12}(T)$ can be obtained for the tandem pore structure in Figure 2 by separately calculating the times for the three segments of the pore in Figure 2 and adding them. Thus

$$E_{12}(T) \approx E_{121}(T) + E'(T) + E_{122}(T) \qquad (10)$$

Table 3 shows the result for the six analytes in Table 1: dAMP at pH=7, A at pH=11, R at pH=7, C at pH=9, H at pH=11, and Y at pH=10..

Table 3. Rough estimate of mean translocation time based on Equation 10 through tandem pore of Figure 2 with $L_{121} = L_{122} = 5$ nm and L' = 1 nm; pore diameter = 3 nm. Voltage profile is of the form (positive voltage, voltage over conductor layer, negative voltage); see Figure 2.

Analyte molecule	pH	Voltage profile	Translocation time (ms)
dAMP	7	(0.4,0,-0.4)	1.34
Alanine	11	(0.4,0,-0.4)	0.725
Arginine	7	(-0.4,0,0.4)	0.961
Cysteine	9	(0.4,0,-0.4)	4.70

Histidine	11	(0.4,0,-0.4)	0.509
Tyrosine	10	(0.4,0,-0.4)	5.90

Writing the tandem pore structure as [*cis* : poreneg : connector : porepos : *trans*], this five-stage structure presents a finite one-dimensional continuum to an analyte. The latter has to negotiate its way across four interfaces: *cis* : poreneg, poreneg : connector, connector : porepos, and porepos : *trans*. Because of diffusion the analyte oscillates at each interface, thus delaying the translocation process. Because diffusion has an approximately gaussian distribution of translocation times, an analyte may be found after a given time in any of the five segments of the pore structure given above. One way to get time estimates would be to formulate a discontinuous F-P equation for the five-stage pore structure and solve it numerically. Here an alternative approach based on simulation is taken.

4. Simulation experiments and results

The slowdown process described above with the tandem pore of Figure 2 was simulated by assuming an analyte molecule to be a dimensionless particle. The simulation procedure is similar to those in [21] and [22]. The details can be accessed in the Supplement. The following analytes were used in the simulations: 1) dAMP, 2) Arginine, and 3) Alanine at two different values of pH. dAMP represents all five nucleotides, Arginine represents the AA subset {R, K, D, E, C, H, Y}, and Alanine the AA subset {A,N,Q,G,I,L,M,F,P,S,T,W,V}.

Table 4 below shows dwell or translocation times for the three analytes with three voltage profiles. When an analyte finds itself in the pore under the influence of the bilevel pore voltage it may oscillate between *cis* and the pore, stay for extended times inside the pore, or translocate fully to exit into *trans*. When no translocation occurs a run is terminated when the total number of steps reaches 2×10^9. When translocation does occur the larger of the dwell time and the translocation time through the pore is used as the measure of slowdown. In the absence of full translocation the longest dwell time of the analyte during the simulation run is used. Full translocation is not a requirement in the model of analyte detection/identification used here. Thus where there is no full translocation and exit into *trans*, an analyte could remain trapped inside the pore for sufficiently long times that the detector can detect the occurrence of a blockade in the pore current and measure the size of the blockade with adequate measurement precision. As can be seen in Table 4, in order to get millisecond-level translocation times it is necessary to increase the positive voltage segment of the profile so that the analyte goes deep into the pore and thereby increases its dwell time. Figure 3 is a bar chart showing the increases in translocation times; note how the time for Alanine jumps by 4 orders of magnitude when the pH value goes from 7 to 11.

Table 4. Increase in translocation times due to three different voltage profiles for three different analytes

Voltage profile	**Translocation time (ms)**			
	dAMP (pH=7)	**Arginine (pH=7)**	**Alanine (pH=7)**	**Alanine (pH=11)**
(0.15,0,-0.5)	7.43×10^{-3}	6.86×10^{-3}	2.15×10^{-5}	4.89×10^{-3}
(0.25,0,-0.5)	0.0909	0.0540	2.32×10^{-5}	0.0413
(0.35,0,-0.5)	1.45	0.361	2.98×10^{-5}	0.154

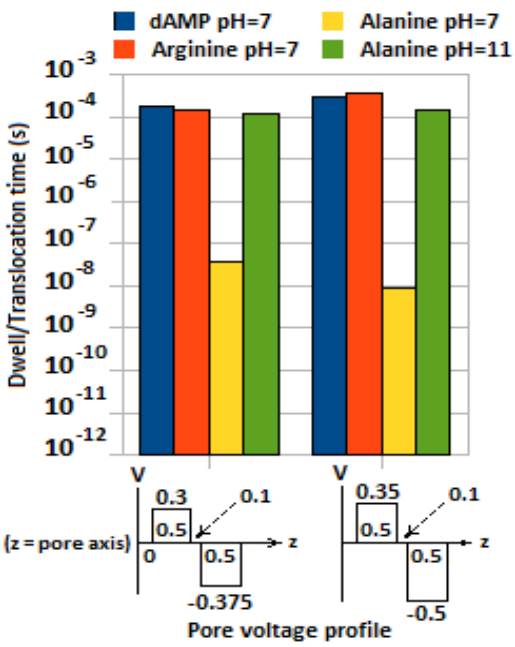

Fig 3. Graphic equivalent of Table 3. a = 1-a = 0.5, b = 0.1, and L_{12} = 11 nm, where a, b, and L_{12} are as in Figure 1e. Voltage axis is in volts; time data correspond to larger of dwell time and translocation time through pore.

5. Effect of bi-level voltage profile on the ionic current

An unintended consequence of the bi-level voltage profile is that it also affects the cations and anions responsible for the pore ionic current I_{pore}. I_{pore} has four components: the currents due to K+ and Cl- ions moving forward from *cis* to *trans* (c→t) and the corresponding reverse currents from *trans* to *cis* (t→c). One can write

$$|I_{pore}| = |I_{Cl-,c\to t} - I_{Cl-,t\to c}| + |I_{K+,t\to c} - I_{K+,c\to t}| \quad (11)$$

The decrease can be estimated from the corresponding translocation/dwell times of ions in the pore. Table 5 below shows the current level due to Cl- ions flowing from *cis* to *trans*, which results in a net decrease in the current. As the normal K+ ion flow from *cis* to *trans* is small the effect of the voltage profile on it is much smaller. A decrease similar to that with Cl- going from *cis* to *trans* occurs in the K+ current from *trans* to *cis*. Since the current delivered by an ion from *cis* to *trans* is inversely proportional to the translocation time through the pore that separates the two chambers the result is a steep fall in the current to ~10% of that without the opposing voltage.

Table 5. Shows increased translocation times of ions in a tandem pore with positive-negative voltage profile of the form (positive voltage segment, conductor layer, negative voltage segment). Pore length = 11 nm.

Voltage profile	**Translocation time with voltage profile (10^{-8} s)**		**Normal pore voltage**	**Translocation time at normal pore voltage (10^{-8} s)**	
(V, V, V)	Cl-	K+		Cl-	K+
(0.5,0,-0.12)	5.83	5.98	0.15	0.55	0.57
(0.5,0,-0.15)	12.4	12.6	0.25	0.85	0.88
(0.5,0,-0.1)	3.69	3.79	0.35	0.41	0.420

6. Discussion

The following are some observations about the slowdown method introduced above.

1) The method presented is fairly straightforward as it does not require any special devices or chemicals. The only extra requirement is constructing two pores in tandem with a conducting layer in between for use as a terminal between the two voltage levels (Figure 2b). This can be done more easily with solid-state pores than with biological pores. Furthermore, voltages can be higher with the former, whereas with a biological pore they are limited by electrical breakdown to about 300 mV, which is too low to allow significant slowdowns. This is also borne out by the simulation results in Table 3, which show that -400 mV or more is required in the negative voltage segment to get translocation times in the millisecond range..

2) As noted above the reduction in the pore current due to a bi-level voltage profile across the tandem pore poses a problem in blockade-based detection of an analyte. In those cases where the pore current is not of a sufficient strength, other methods may be appropriate. Thus by labeling the analyte with a fluorophore its delayed passage through the pore with the bi-level voltage profile can be detected optically independent of the pore current value. For example, in [23] a fluorophore-labeled molecule passes from the unlit (dark) *cis* side of an e-cell to the lighted *trans* side where it emits light and is detected.

3) With AAs since different pH values are used to achieve slowdown, they need to be probed in different e-cells. A method to separate AAs from a sample by routing them to 20 different e-cells (one for each of the 20 different AAs) is described in [24]. It enables unambiguous separation of AAs such that with detection based on current blockades it suffices to merely detect the presence of an AA in the pore without having to know the size of the blockade. This is a binary measurement, it does not require precise measurement of the current blockade level. This effectively converts AA detection from a high precision analog process to a low precision digital one. If optical detection with fluorophore labels is used then a single color can be used for all 20 AAs.

4) Analyte translocation is a stochastic phenomenon so there is no guarantee that an analyte will enter the pore within a reasonable amount of time. One recent method [18] uses a nanopipette to trap short DNA strands for transfer to a detector like a nanopore. Here a different approach based on the use of hydraulic pressure [25] has been used in all the simulations. Thus a piston at the top of *cis* with a pressure of ΔP on it results in flow of the analyte to and through the pore; see Figure S-2 in the Supplement. In the simulations described earlier the use of hydraulic pressure results in an analyte introduced into the top of cis reaching the pore entrance without fail. There is, however, a tradeoff: the use of hydraulic pressure also prevents the flow of ions from *trans* to *cis*, thereby effectively halving the pore current (see Equation 11).

5) An analyte may be trapped multiple times inside the pore. All sufficiently long dwells can then be recorded by the detector to increase the confidence level of the measurement. With n such dwells, such multiple reads can be thought of as providing nX coverage.

Supporting Information. Supplementary file containing mobility and diffusion coefficient data, additional information on the F-P model, and simulation details.

References

[1] L. Reynaud, A. Bouchet-Spinelli, C. Raillon, and A. Buhot, "Sensing with nanopores and aptamers: a way forward", *Sensors* **20**, 4495, 2020. doi:10.3390/s20164495

[2] D. Deamer, M. Akeson, and D. Branton, "Three decades of nanopore sequencing". *Nat. Biotechnol*. **34**, 518–524, 2016.

[3] N. Callahan, J. Tullman, Z. Kelman, and J. Marino. "Strategies for development of a next-generation protein sequencing platform". *Trends Biochem. Sci*. 2019. doi:10.1016/j.tibs.2019.09.005.

[4] G. Sampath. "Amino acid discrimination in a nanopore and the feasibility of sequencing peptides with a tandem cell and exopeptidase". *RSC Adv*., **5**, 30694–30700, 2015.

[5] P. Boynton and M. Di Ventra. "Sequencing proteins with transverse ionic transport in nanochannels". *Sci. Rep*., **6**, 25232, 2016.

[6] Y. Zhao, B. Ashcroft, P. Zhang, H. Liu, S. Sen, W. Song, J. Im, B. Gyarfas, S. Manna, S. Biswas, C. Borges, and S. Lindsay. "Single-molecule spectroscopy of amino acids and peptides by recognition tunneling". *Nature Nanotechnol*., 9, 466–473, 2014.

[7] E. Kennedy, Z. Dong, C. Tennant, and G. Timp. "Reading the primary structure of a protein with 0.07 nm^3 resolution using a subnanometre-diameter pore". *Nature Nanotechnol*. , **11**, 968–976, 2016.

[8] H. Ouldali, K. Sarthak, T. Ensslen, F. Piguet, P. Manivet, J. Pelta, J. C. Behrends, A. Aksimentiev, and A. Oukhaled, "Electrical recognition of the twenty proteinogenic amino acids using an aerolysin nanopore", *Nature Biotech*., **38**, 176–181, 2020. doi: 10.1038/s41587-019-0345-2 (Reviewed in: S. Howorka and Z. S. Siwy, "Reading amino acids in a nanopore", *Nature Biotechnol*., 38, 159–160, 2020. doi: 10.1038/s41587-019-0401-y)

[9] W. Si, Y. Zhang, G. Wu, Y. Kan, Y. Zhang J. Sha, and Y. Chen, "Discrimination of protein amino acid or its protonated state at single-residue resolution by graphene nanopores", *Small*, 2019. doi: 10.1002/smll.201900036

[10] D. Fologea, J. Uplinger, B. Thomas, D. S. McNabb, and J. Li, "Slowing DNA Translocation in a Solid State Nanopore", *Nano Lett*., **5**, 1734-1737, 2005. doi:10.1021/nl051063o

[11] R. Samanthi, S. de Zoysa, D. A. Jayawardhana, Q. Zhao, D. Wang, D. W. Armstrong, and X. Guan, "Slowing DNA translocation through nanopores using a solution containing organic salts", *J. Phys. Chem. B*, **113**, 13332–13336, 2009.

[12] S. W. Kowalczyk, D. B. Wells, A. Aksimentiev, and C. Dekker, "Slowing down DNA translocation through a nanopore in lithium chloride", *Nano Lett*., **12**, 1038-1044, 2012. doi:1 0.1021/nl204273h

[13] J. Feng, K. Liu, R. D. Bulushev, S. Khlybov, D. Dumcenco, A. Kis, and A. Radenovic, "Identification of single nucleotides in MoS2 nanopores", *Nature Nanotech*., 2015. doi: 10.1038/nnano.2015.219

[14] W. Si, Y. Zhang, J. Sha, and Y. Chen, "Controllable and reversible DNA translocation through a single-layer molybdenum disulfide nanopore", *Nanoscale*, **10**, 19450-19458, 2018. doi: 10.1039/c8nr05830j

[15] J. Larkin, R. Henley, D. C. Bell, T. Cohen-Karni, J. K. Rosenstein, and M. Wanunu, "Slow DNA transport through nanopores in hafnium oxide membranes", *ACS Nano*, **7**, 10121–10128, 2013.

[16] K. R. Lieberman, G. M. Cherf, M. J. Doody, F. Olasagasti, Y. Kolodji, and M. Akeson, "Processive replication of single DNA molecules in a nanopore catalyzed by phi29 DNA polymerase", *J. Am. Chem. Soc*., **132**, 17961–17972, 2010. doi: 10.1021/ja1087612

[17] Z. Yuan, Y. Liu, M. Dai, X. Yi, and C. Wang, "Controlling DNA translocation through solid-state nanopores", *Nanoscale Res. Lett*., **15**, 2020. doi: 10.1186/s11671-020-03308-x

[18] K. J. Freedman, L. M. Otto, A. P. Ivanov, A. Barik, S.-H. Oh, and J. B. Edel. "Nanopore sensing at ultra-low concentrations using single-molecule dielectrophoretic trapping". *Nature Commun*., **7**, 10217, 2016. doi: 10.1038/ncomms10217

[19] D. L. Nelson and M. M. Cox, *Lehninger's Principles of Biochemistry*, 4th edn., 2005, W H Freeman.

[20] D. Y. Ling and X. S. Ling, "On the distribution of DNA translocation times in solid-state nanopores: An analysis using Schrödinger's first-passage-time theory", *J. Phys. Cond. Matter*, 2013. doi: 10.1088/0953-8984/25/37/375102

[21] G. Sampath. "DNA sequencing with stacked nanopores and exonuclease: a simulation-based analysis". *Electrophoresis,* 37, 2429-2434, 2016. doi: 10.1002/elps.201600049

[22] K. T. Brady and J. E. Reiner, "Improving the prospects of cleavage-based nanopore sequencing engines", *J. Chem. Phys*., **143**, 074904, 2015.

[23] N. Klughammer and C. Dekker, "Palladium zero-mode waveguides for optical single molecule detection with nanopores", *Nanotech*., 2021. doi: 10.1088/1361-6528/abd976

[24] G. Sampath, "Label-free amino acid identification for de novo protein sequencing via tRNA charging and current blockade in a nanopore", *bioRxiv*, 2020.06.25.170803. doi:10.1101/2020.06.25.170803

[25] B. Lu, D. P. Hoogerheide, Q. Zhao, H. Zhang, Z. Tang, D. Yu, and J. A. Golovchenko. "Pressure-controlled motion of single polymers through solid-state nanopores". *Nano Lett*., **13**, 3048–3052, 2013.